Fitting of NWM Ray-Traced Slant Factors to Closed-Form Tropospheric Mapping Functions

102

Landon Urquhart, Marcelo Santos, and Felipe Nievinski

Abstract

In this paper we investigate the fitting of ray-tracing results to closed-form expressions. We focus on the variation of the delay with elevation angle and azimuth. For the elevation angle-dependence we compare the continued fraction form of Yan and Ping (Astron J 110(2):934–993, 1995) with that of Marini (Radio 11 Sci 7(2):223–231, 1972) (normalized to yield unity at zenith and found negligible differences between the two functional formulations for the hydrostatic case, while for the non-hydrostatic case, the Yan and Ping model performed marginally better. Since the ray-tracing results do not necessarily assume azimuthal symmetry, we have to account for the azimuth-dependence. For that we compare the linear gradient model of Davis et al. (Radio Sci 28(6):1003–1018, 1993) with the inclusion of second order terms (Seko et al., J Meteorol Soc Jpn 82 (1B):339–350, 2004) and arbitrary spherical harmonics. These functional forms performed very well for the hydrostatic case, although for the non-hydrostatic case there were some large biases, particularly in the spherical harmonics of order 1, degree 1 and the 2nd order polynomial case.

102.1 Introduction

As electromagnetic signals propagate through the atmosphere they experience path delays due to the electrically neutral atmosphere. At the zenith, this delay roughly has a magnitude of 2.3 m (at sea level) and can grow to tens of meters near the horizon (Langley 1998). The ultimate goal in geodesy is to *mitigate* the tropospheric delay, in order to remove any bias from the resulting position estimates. To model the tropospheric delay, it is convenient to separate the delay into a hydrostatic and a non-hydrostatic component contributing to the delay experienced in the zenith direction. A mapping function then models the elevation dependence of the tropospheric delay:

$$\Delta L(\varepsilon) = \kappa_{\mathrm{h}}(\varepsilon) \cdot \Delta L_h^z + \kappa_{nh}(\varepsilon) \cdot \Delta L_{\mathrm{nh}}^z \qquad (102.1)$$

where ΔL is the total along path delay, κ_{h} and κ_{nh} are the hydrostatic and non-hydrostatic mapping functions dependent only on elevation angle, ΔL_k^z and ΔL_{nk}^z are the hydrostatic and non-hydrostatic zenith delay and ε the elevation angle of the satellite.

L. Urquhart (✉) • M. Santos
Department of Geodesy and Geomatics Engineering, University of New Brunswick, P.O. Box 4400, Fredericton, NB, Canada E3B 5A3
e-mail: landon.u@unb.ca

F. Nievinski
Department of Aerospace Engineering Sciences, University of Colorado, Boulder, CO 80309-0429, USA

S. Kenyon et al. (eds.), *Geodesy for Planet Earth*, International Association of Geodesy Symposia 136,
DOI 10.1007/978-3-642-20338-1_102,

Various elevation angle-dependent mapping functions have been suggested in the past, many which were systematically tested by Mendes (1999), although under the assumption of a spherically symmetric atmosphere. With the improvement of space geodetic observations, the asymmetric nature of the atmosphere has been shown to have an impact on the resulting station position (MacMillan 1995). This has led to the development of mapping functions which attempt to model the variation of the delay, not only as a function of elevation angle, but also as a function of azimuth.

The purpose of this contribution will be to compare the functional forms used in tropospheric delay modeling. Rather than focus on specific mapping functions, we work with the functional forms themselves in order to identify which ones provide the most realistic representation of the tropospheric delay.

The end goal of this research is to identify the most realistic models of the tropospheric delay, expressed in a convenient closed-form manner, which can then be used to either predict or estimate the effect of tropospheric delay in space geodetic data analysis.

102.2 Decomposing the Delay

Following Nievinski (2009), the tropospheric delay in its most general form, is a function of date and time (t), receiver location (latitude ϕ, longitude λ, and height h) and satellite location given in the topocentric frame (elevation angle ε, and azimuth α):

$$\Delta L = f(t,\, \phi,\, \lambda,\, h,\, \varepsilon,\, \alpha). \tag{102.2}$$

The delay is most often decomposed as:

$$\Delta L = \Delta L^z \times k \tag{102.3}$$

where ΔL^z is the zenith delay, defined as:

$$\Delta L^z = f(t,\, \phi,\, \lambda,\, h,\, \varepsilon = 90^\circ,\, \alpha). \tag{102.4}$$

In this way, the variation of the slant delay to a given satellite is confined to the slant factor, $k = \frac{\Delta L}{\Delta L^z}$, a unitless ratio. A mapping function can then be described as a model for the variation of the slant factor values with respect to the independent variables. This allows us to distinguish between the slant factor model or mapping function (denoted κ) from a particular slant factor value (denoted k), resulting from the evaluation of the former at a specific epoch $(t = t')$, position $(\phi = \phi',\, \lambda = \lambda',\, h = h')$, and direction $(\varepsilon = \varepsilon',\, \alpha = \alpha')$:

$$k = \kappa(t',\, \phi',\, \lambda',\, h',\, \varepsilon',\, \alpha') \tag{102.5}$$

It is helpful to further distinguish between the functional form (Boehm and van Dam 2009) and the realization of a mapping function. The functional form describes how the slant factor varies with respect to some parameter. The most common functional form in use today is Marini's (1972) continued fraction expansion of $\frac{1}{\sin(\varepsilon)}$, normalized to yield unity at zenith, as given by Herring (1992):

$$\kappa(\varepsilon) = \cfrac{1 + \cfrac{a}{1 - \cfrac{b}{1 - \cfrac{c}{\cdots}}}}{\sin(\varepsilon) + \cfrac{a}{\sin(\varepsilon) + \cfrac{b}{\sin(\varepsilon) + \cfrac{c}{\cdots}}}} \tag{102.6}$$

The variation with respect to azimuth is, most of the time, neglected, and sometimes accounted for with a single main direction of asymmetry (Davis et al. 1993):

$$\delta\kappa\,(\varepsilon, \alpha) = \kappa_0(\varepsilon)\cot(\varepsilon)\,[G_N\,\cos(\alpha) + G_E \sin(\alpha)] \tag{102.7}$$

where k_0 represents the symmetric mapping function, G_N and G_E are the north and east coefficients describing the direction and magnitude of asymmetry exhibited by slant factors and α is the azimuth of the observation.

The realization of the mapping functions described in (102.6) and (102.7) can take several different forms as shown in Niell (1996) and Boehm et al. (2006). The troposphere gradient terms, G_N and G_E can also be determined by using a profile method (Boehm and Schuh 2007) or three dimensional ray-tracing (Chen and Herring 1997) and it is also possible to have various gradient mapping functions k_0.

So it can be seen that although the underlying functional forms for the mapping functions described above are the same, the realization of those models are quite different. The comparison can become even more complex if we consider mapping functions which require the use of external parameters directly in the mapping functions such as the generator function method described in Yan and Ping (1995).

Due to these differences in the realization of the functional forms, the evaluation is typically of the mapping function itself, as is the case for Mendes (1999). In order to avoid this downfall, we use a homogenous approach to both derive the mapping functions based on the functional forms as well as in the evaluation.

102.3 Functional Formulations

Various functional formulations have been developed over the years to describe both the elevation angle- and azimuth- dependence of the tropospheric delay. Table 102.1 shows the functional forms tested along with the number of coefficients to be estimated. For those functional forms which consider the atmosphere to by symmetrical, we have compared Marini's (1972) continued fraction form, described in (102.6), for both the 3 coefficient expansion and the 4 coefficient expansion, Yan and Ping's (1995) generator function method and the simplification of Marini's (1972) expression using empirical values for the *b* and *c* coefficients as done in the Vienna Mapping Functions (VMF) described in Boehm et al. (2006). To ensure consistency with the truth values, the *a* coefficient in the VMF was calculated using the same ray-tracing scheme as the other models, although under the assumption of spherical osculating atmosphere, to be consistent with the approach used in Boehm et al. (2006).

For the asymmetric delay, the standard, linear gradient formulation described in Davis et al. 1993 was compared to the 2nd order polynomial expansion developed by Seko et al. (2004) as well as the possibility of using spherical harmonics as described in Boehm and Schuh (2001).

102.4 Experiment Description

The atmospheric parameters required for three dimensional ray-tracing were obtained through the Canadian Regional NWM, produced by the Canadian Meteorological Center (CMC). This NWM has a spatial resolution of 15 km horizontally, and contains 28 isobaric levels plus a surface level.

Although at this resolution small scale perturbations which may be due to cloud like structures are not detectable, larger scale "gradient like" structures in the troposphere have been shown to be detectable (Davis et al. 1993). As these small scale perturbations fluctuate rapidly it would be more appropriate to treat them with a statistical model rather than attempt to model them in the functional form. That said, the use of a finer mesh NWM, may lead to further insights into the accuracy of the functional forms.

A site-specific approach, similar to the approach used for the rigorous VMF1 site, was followed (Boehm et al. 2006). A total of 29 ray-traced observations at elevation angles of (3°, 4°, 6°, 8°, 14°, 30°, 70° and 90°) and azimuths of (0°, 90°, 180° and 270°) were used to estimate the coefficients through a least squares procedure.

To evaluate the functional forms, truth values computed at a regularly spaced interval of 15° in

Table 102.1 Functional formulations and coefficients

Formulation	Number of unknowns	Coefficients
Marini 3 coefficient	3	a, b, c
Marini 4 coefficient	4	a, b, c, d
Yan and Ping	4	d_1, d_2, d_3, d_4
Modified VMF	1	a (UNB ray-tracing scheme to determine "a")
Linear gradient model	5	a, b, c, G_N, G_E
Spherical harmonics	3 + harmonic coefficients	a, b, c, a_{10}, a_{11}, b_{11}, . . . , a_{nm}, b_{nm}
2nd order polynomial	8	a, b, c, G_N, G_E, G_{NN}, G_{EE}, G_{NE}

azimuth and at elevation angles of 3°, 5°, 7° and 10° were computed. The truth values as well as the fitted values were determined for every 5th day of 2008 at epoch 00:00h UTC, for station CAGS located in Gatineau, Canada, totalling 73 days.

Slant factors were computed, using (102.3) for the truth and fitted observations. The difference between the slant factors were then multiplied by a nominal 2.3 m for the hydrostatic and 0.22 m for the non-hydrostatic to obtain the error of the delay in units of meters.

102.5 Results and Discussion

The residuals of the least squares estimation for each formulation were sorted by elevation angle and the mean and standard deviation computed. For the modified VMF, there was no estimation involved so it is not included in the residual analysis. Figure 102.1 shows the mean of the residuals for the hydrostatic mapping functions. The largest bias of the symmetric mapping functions is present in the Marini four coefficient expression while the Yan and Ping expression exhibits a bias which is larger at higher elevation angles but seems to perform better than the Marini three coefficient model at the low elevation angles, although the differences are marginal. The standard deviations at each elevation angle, shown in Table 102.2, are very similar for all three symmetric cases which was expected as they are unable to model the azimuthal variation of the tropospheric delay.

The asymmetric mapping functions exhibit biases of similar magnitude as the Marini 3 coefficient when binned by elevation. This is expected as the Marini 3 coefficient expression is part of the formulation used in the asymmetric mapping functions (k_0). The standard deviations shown in Table 102.2 shows that above 14° elevation angle there is really no benefit to using the asymmetric functional forms over the symmetric expressions. As we move to lower elevation angles, we start to see the improvement in the fit of the asymmetric expressions, especially in the standard deviation which is much smaller for the asymmetric cases.

Next we consider the bias present between the truth observations and those computed using the derived mapping functions described above. Figure 102.2 shows that the Marini 3 coefficient model performs very well, exhibiting nearly a zero bias for the hydrostatic case. There appears to be no significant change to adding a fourth coefficient to the Marini expression.

The mVMF, which uses empirical values for the 2nd and 3rd coefficient in the Marini expression, has a small bias but, even at 5° it is less than 1 cm, which again confirms the validity of using this approach for high accuracy applications. The biases are comparable for the asymmetric case. The real advantage of the asymmetric models can be seen in the standard deviations, shown in Table 102.3. For the spherical harmonics model, the standard deviation at the 5°

Table 102.2 Standard deviations of the residuals for the fitting of the functional forms to the ray-traced hydrostatic delay (units = mm)

Formulation	Elevation angle						
	3°	4°	6°	8°	14°	30°	70°
Marini 3 coefficient	57.2	41.8	24.0	15.1	5.6	1.4	0.1
Marini 4 coefficient	57.2	42.3	24.2	16.2	6.8	1.6	0.1
Yan and Ping	57.2	41.8	24.0	15.1	5.6	1.4	0.1
SH11	31.8	18.3	9.4	10.6	4.3	1.2	0.1
SH21	13.1	8.0	5.5	15.7	5.7	1.4	0.1
2nd order polynomial	5.1	4.0	6.0	4.8	2.1	0.7	0.1
Linear grad.	13.4	8.6	6.9	5.2	2.6	1.0	0.1

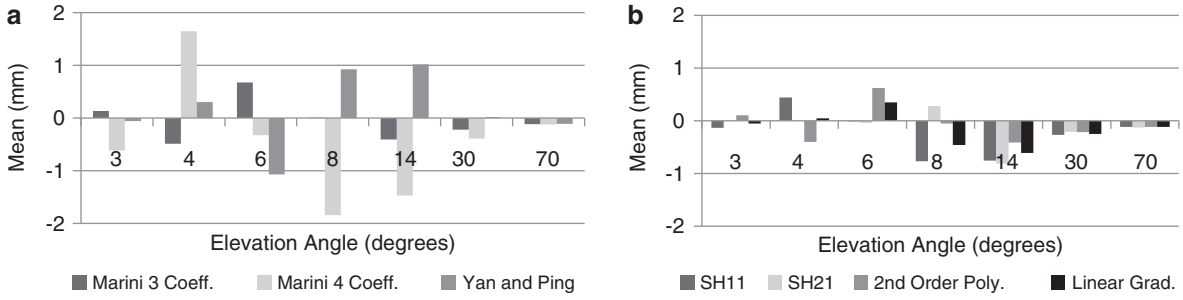

Fig. 102.1 Hydrostatic Residuals binned by elevation angles: (**a**) symmetric; (**b**) asymmetric

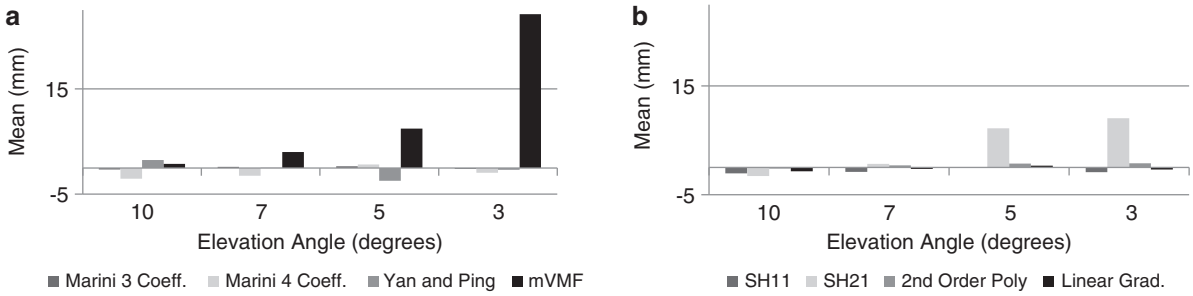

Fig. 102.2 Discrepancy between truth and mapped hydrostatic delay: (**a**) symmetric; (**b**) asymmetric

Table 102.3 Standard deviation of the hydrostatic delay biases between the truth and mapped observations (units = mm)

Formulation	Elevation angle			
	10°	7°	5°	3°
Marini 3 coefficient	10.5	19.4	32.2	58.8
Marini 4 coefficient	12.0	20.0	32.3	58.9
Yan and Ping	10.5	19.3	32.2	58.8
mVMF	10.8	19.8	32.8	59.5
SH11	2.8	7.9	17.1	36.7
SH21	6.2	4.9	6.9	17.6
2nd order polynomial	9.3	19.0	37.3	104.1
Linear grad.	5.8	12.2	26.2	82.2

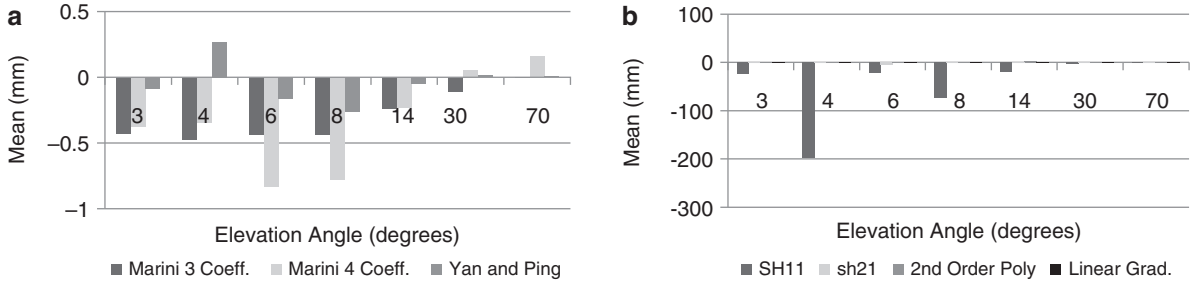

Fig. 102.3 Non-hydrostatic residuals binned by elevation angles: (**a**) symmetric; (**b**) asymmetric

elevation angle improves from 32.2 mm for the symmetric functional forms down to 6.9 mm for spherical harmonics of degree 2 and order 1 (SH21).

Although the 2nd order polynomial performed well in the residual analysis, we see that it performed the worst out of all of the asymmetric formulations. This may be due to the number of azimuths used in the observation scheme. If the number of azimuths used to fit the models were increased from four to eight it is expected that we would see an improvement in the results.

Figure 102.3 shows the non-hydrostatic results. For the symmetric mapping functions there is a bias of less than 1 mm, which can be considered negligible. Although the Yan and Ping functional form was not originally intended for non-hydrostatic use it did perform well, having the smallest mean at most elevation angles. We did see a small improvement at low elevation angles as well as for the Marini 4 coefficient model, although the slight improvement does not justify the added complexity of a fourth coefficient in the estimation process.

For the asymmetric case there was a large bias for spherical harmonics of, degree 1, order 1 (SH11) while the other mapping functions performed similar to the

Table 102.4 Standard deviation of the residuals for fitting the functional forms to the non-hydrostatic delay (units = mm)

Formulation	Elevation angle						
	3°	4°	6°	8°	14°	30°	70°
Marini 3 coefficient	148.3	106.2	60.5	38.0	13.9	3.1	0.3
Marini 4 coefficient	148.3	106.2	60.5	38.0	13.9	3.2	0.6
Yan and Ping	148.2	106.1	60.4	37.9	13.8	3.1	0.3
SH11	79.0	95.5	26.8	39.8	13.3	2.8	0.1
SH21	22.3	14.5	14.1	39.4	14.3	3.2	0.1
2nd order polynomial	8.1	7.8	8.6	7.2	7.0	3.4	0.6
Linear grad.	24.6	17.1	18.2	13.9	6.0	1.6	0.2

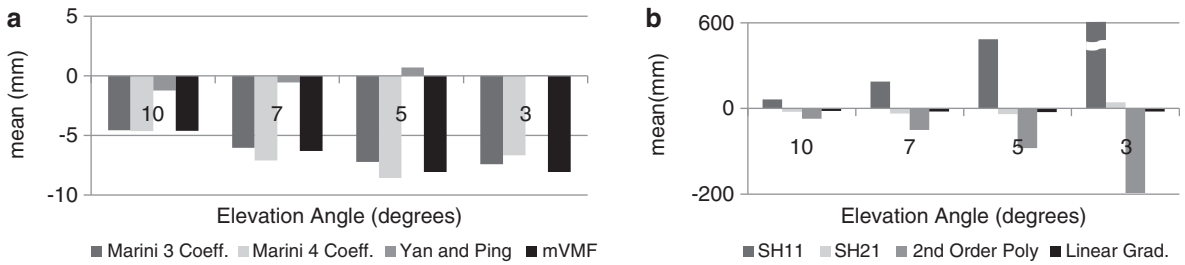

Fig. 102.4 Discrepancy between truth and mapped non-hydrostatic delay: (**a**) symmetric; (**b**) asymmetric

symmetric mapping functions. The real improvement once again came when considering the standard deviations, shown in Table 102.4, which for the asymmetric mapping functions were much lower than the symmetric cases. The 2nd order model performed the best with an 8 mm standard deviation at 3° while the symmetric mapping functions exhibited a standard deviation of nearly 148 mm. Once again, for higher elevation angles above 15° there is no advantage to using the asymmetric models.

For the non-hydrostatic case the bias for the three coefficient Marini expression based mapping functions are very similar to the mVMF (Fig. 102.4). The bias is typically around 7 mm. For the Yan and Ping formulation the bias is much better typically less than 1 mm.

For the asymmetric expressions we see that now a bias appears in SH11 at low elevation angles. This is similar to the residual analysis which saw poor performance in the case of SH11. SH21 and the standard linear gradient formulation performed the best both having biases of about 1 cm at 3° elevation angle. The 2nd order polynomial, which performed very well in the residual analysis, was not able to adequately model the variation of the delay with respect to azimuth and large discrepancies were seen. Once again this may be a result of the low number of azimuths used in the estimation of the coefficients.

102.6 Conclusion and Future Work

Closed-form mapping functions will continue to play an important role in the processing of space geodetic data for years to come. By using three dimensional ray-tracing through a NWP model it was possible to test some of the most common mathematical models in use today.

In this contribution we choose to put the time-variation of the tropospheric delay out of the scope and focus on developing site and epoch specific mapping functions, similar to the manner used in the VMF1-site.

Both symmetric and asymmetric formulations were tested. It was found that all of the symmetric mapping functions tested were able to adequately model the elevation angle dependence of the tropospheric delay above an elevation angle of 14°. Even using empirical values for several of the coefficients as done for the VMFs only introduced a slight bias and at elevation angles below 5°. However, since they do not consider the variation with respect to azimuth they possess large standard deviations. On the other hand, the use of spherical harmonics was shown to be an improvement over other models such as the standard linear gradient expression and the 2nd order polynomial model.

For the non-hydrostatic delay, the Yan and Ping formulation performed very well exhibiting only a small bias in elevation angle where as the Marini expressions had a bias of nearly 8 mm. The asymmetrical models on the other hand experienced some difficulty and were not able to properly model the delay to the degree that was expected. Further research will need to be done to identify the problem, but by including more observations at different azimuths it is believed it would improve the fit of the models. Also experimenting with different gradient mapping functions, such as those suggested by Chen and Herring (1997) should be attempted. It is also necessary to expand the test locations to include more stations at various latitudes and elevations.

Acknowledgements The authors would like to thank the Natural Sciences and Engineering Research Council of Canada for funding this research. The last author would also like to acknowledge funding provided by CAPES/Fulbright.

References

Boehm J, Schuh H (2001) Spherical harmonics as a supplement to global tropospheric mapping functions and horizontal gradients. In: Behrend D, Rius A (eds) Proceedings of the 15th working meeting on European VLBI for geodesy and astrometry, Barcelona, 7–8 September, pp 143–148

Boehm J, Schuh H (2007) Troposphere gradients from the ECMWF in VLBI analysis. J Geod 81:403–408

Boehm J, Van Dam T (2009) Modelling deficiencies and modelling based on external data. Second GGOS unified analysis workshop, San Francisco, CA, 11–12 December

Boehm J, Werl B, Schuh H (2006) Troposphere mapping functions for GPS and very long baseline interferometry from European Centre for Medium-Range Weather Forecasts operational analysis data. J Geophys Res 111:B02406

Chen G, Herring TA (1997) Effects of atmospheric azimuth asymmetry on the analysis of space geodetic data. J Geophys Res 102(B9):20489–20502

Davis JL, Elgered G, Niell AE, Kuehn CE (1993) Ground-based measurement of gradients in the "wet" radio refractivity of air. Radio Sci 28(6):1003–1018

Herring TA (1992) Modelling atmospheric delays in the analysis of space geodetic data. In: de Munck JC, Th. Spoelstra TA (eds) Proceedings of the symposium refraction of transatmospheric signals in geodesy, No. 36, Netherlands Geodetic Commission, The Hague, pp 157–164

Langley RB (1998) Propagation of the GPS signals. In: Teunissen PJG, Kleusberg A (eds) GPS for geodesy, 2nd edn. Springer, Berlin, pp 112–149

MacMillan DS (1995) Atmospheric gradients from very long baseline interferometry observations. Geophys Res Lett 95 (9):1041–1044

Marini JW (1972) Correction of satellite tracking data for an arbitrary tropospheric profile. Radio Sci 7(2):223–231

Mendes VB (1999) Modeling the neutral-atmosphere propagation delay in radiometric space techniques. PhD thesis, Department of Geodesy and Geomatics Engineering, Technical Report 199, University of New Brunswick, Fredericton, NB, April, 349 pp

Niell AE (1996) Global mapping functions for the atmosphere delay at radio wavelengths. J Geophys Res 101(B2): 3227–3246

Nievinski, FG (2009) Ray-tracing options to mitigate the neutral atmosphere delay in GPS. MScE thesis, Technical Report No. 262, Department of Geodesy and Geomatics Engineering, University of New Brunswick, Fredericton, NB, 232 pp. hdl:1882/1050

Seko H, Nakamura H, Shimada S (2004) An evaluation of atmospheric models for GPS data retrieval by output from a numerical weather model. J Meteorol Soc Jpn 82 (1B):339–350

Yan H, Ping J (1995) The generator function method of the tropospheric refraction corrections. Astron J 110(2):934–993